Advances in Turbulence X
Proceedings of the Tenth European Turbulence Conference
H. I. Andersson & P.-Å. Krogstad (Eds.)
©CIMNE, Barcelona 2004

Inclined cross-stream stereo PIV measurements in turbulent boundary layers.

N. Hutchins, W. Hambleton, I. Marusic
Dept of Aerospace Engineering and Mechanics
University of Minnesota, Minneapolis, MN 55455, USA
Contact address: *marusic@aem.umn.edu*

1 Introduction

By arranging the laser light-sheet and image plane of a stereo PIV system in inclined spanwise/wall-normal planes (inclined at both 45° and 135° to the x-axis) we have obtained a unique quantitative view of the turbulent boundary layer in planes aligned both with and against the principle vorticity axis of a proposed hairpin model. These experiments have been repeated across a range of Reynolds numbers ($Re_\tau \approx 800 - 3050$). In-plane swirl results indicate the presence of inclined eddies, arranged about low-speed regions (with circumstantial evidence suggesting that these occasionally group into packet-like formations). Two-point correlations show that outer scaling is the correct way to quantify the characteristic spanwise lengthscale across the range of Re_τ.

2 Facility

Experiments are conducted in an open return suction-type boundary layer wind-tunnel of working section $4.7 \times 1.2 \times 0.3$ m. The basic set-up for the 45° and 135° cases are shown in Figure 1. For both inclined planes, the out-of-plane direction is referred to as x' and the in-plane component of the wall-normal ordinate as z'. Spanwise ordinates are unchanged ($y' = y$). The velocity components along the x', y' and z' axes are denoted as u_θ, v_θ and w_θ respectively, where θ is the image-plane inclination angle. Mean velocity, turbulent intensity and Reynolds shear stress profiles have been compared with results collated in [1], confirming that this application of PIV has successfully resolved the principle features of the turbulent boundary layer. In addition, two-point correlations from the inclined-plane data-sets have been compared with existing PIV data taken in spanwise wall-normal planes, showing excellent agreement between the two cases [2].

3 In-plane Swirl Results

Figures 2(a) & (b) show example instantaneous in-plane swirl patterns for both inclined planes. The 2-D swirl approximation is calculated from v_θ and w_θ. Vorticity is used to recover sign. Darker shaded patches show regions of positive

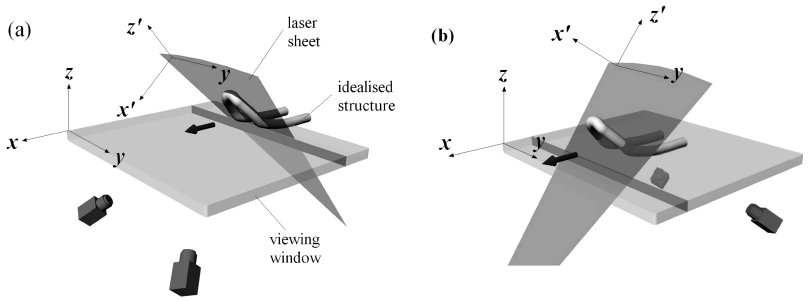

Figure 1: Basic PIV set-up for (a) 45° and (b) 135° cases.

signed swirl, whilst the white areas indicate negative. In-plane vector fields (superimposed over the plots) demonstrate that 2-D swirl is successfully identifying rotating patterns in the flow for these planes. Such patterns are associated with vortex cores piercing the planes (at some oblique angle). It is immediately noticeable that the in-plane swirl is much more prevalent in the 135° plane than the 45°. This is consistent with the observations of Head and Bandyopadhyay [3]. To highlight the disparity in 2-D swirl between the two planes, Figure 2(c) shows the mean swirl calculated for each wall-normal location across the vector field. Averaging across the data-set in this way, there is substantially less in-plane swirling activity in the 45° vector fields. This is consistent with the inclined hairpin vortex and packet models as proposed for the turbulent boundary layer (Adrian and co-workers). Figure 2(d) shows a schematic of this model. Hairpin structures are shown grouped in a packet at inclination angles close to 45°. The two inclined planes bisecting this packet show that such an arrangement would lead to greater in-plane swirling in the 135° plane than the 45° case (if all structures were ideal and aligned at 45° to the x-axis there would be no 2-D swirling evident in the 45° plane). Furthermore, the packet arrangement implies the occasional occurrence in the 135° plane of well-ordered arrangements of positive and negative swirl, stacked above one another, and flanking a region of reduced streamwise momentum. The region labelled (I) in Figure 2(b), is a clear example of such a packet signature (certainly this region is qualitatively similar to the flow pattern shown in the 135° plane of plot d). Similar patterns of positive and negative swirling motions flanking elongated low-speed regions were noted previously in spanwise/streamwise plane PIV results [4][5].

4 Reynolds number scaling

Figure 3(a) illustrates the process by which a characteristic lengthscale is extracted from a two-point correlation (in this instance the spanwise lengthscale is extracted from R_{uu}). We establish a nominal threshold (in this case $th = 0.05$),

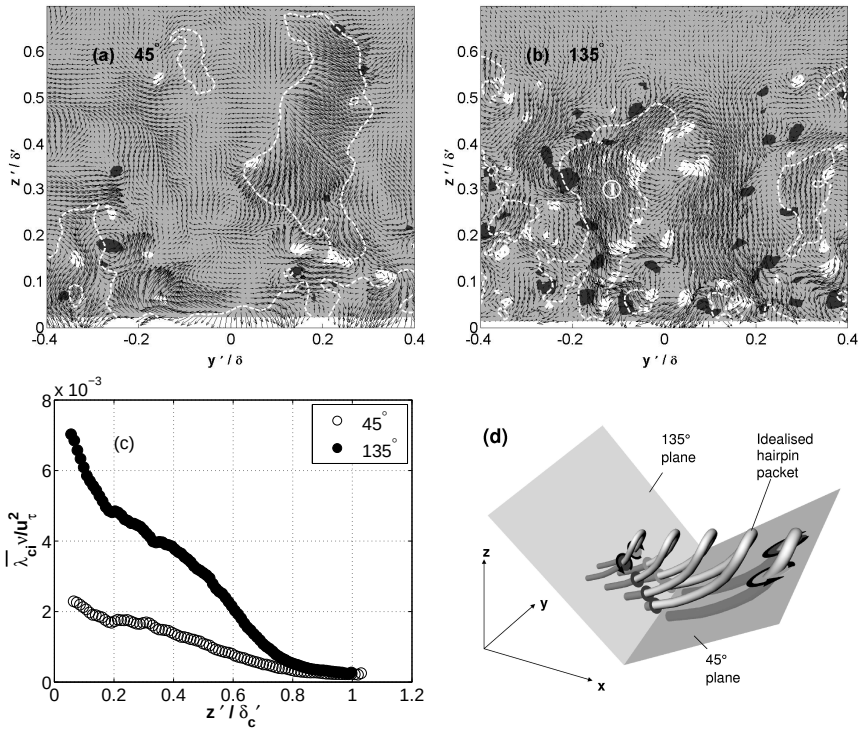

Figure 2: (a) 45° and (b) 135° instantaneous flow-fields ($Re_\tau = 1142$). Shading shows positive and negative signed swirl; (dark) $\lambda_s^+ > 0.02$; (light) $\lambda_s^+ < -0.02$. Vectors shown are v_θ and w_θ. Dashed contours show $u < -u_\tau$; (c) Wall-normal variation of inner-scaled mean swirl. Data averaged across 450 frames at $Re_\tau = 1142$; (d) Schematic rendering of an idealised hairpin vortex packet.

and find the intercept of R_{uu} with this value (width at $z = z_{ref}$ of the largest solid contour in Figure 3 a). This process is repeated for all wall-normal locations (z_{ref}), for both planes and at all Reynolds numbers. The spanwise lengthscales based on R_{uu} are shown in Figure 3(b), where the quality of the collapse for all four Reynolds numbers clearly shows that $l_y(R_{uu})$ scales on outer-variables. A similar collapse is found for $l_y(R_{vv})$ and $l_y(R_{ww})$. Outer scaling of these length-scales was previously proposed by [6] and [7]. It is also noted that these length-scales exhibit an approximately linear growth with z, consistent with the proposed scaling in the attached eddy hypothesis [8].

As a final point, below a given z_{ref}, R_{uu} contours can appear curtailed or splatted onto the wall. This is visible in the 0.05 and 0.15 contours of Figure 3(a), which have a flattened profile (asymmetric about z_{ref}). Beyond a certain z_{ref}, these contours appear to 'lift' or 'separate' from the wall. We tentatively refer

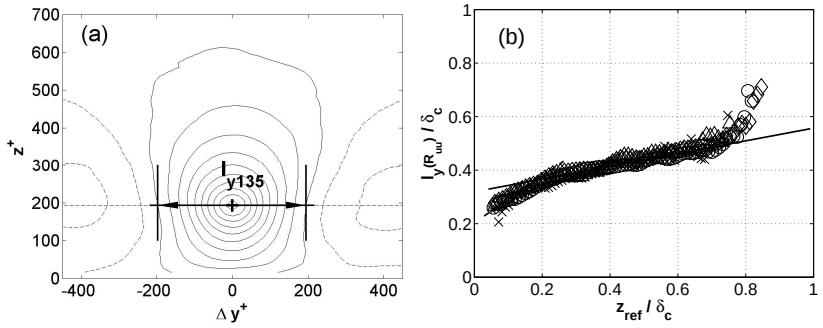

Figure 3: (a) two-point correlation contours of R_{uu} (135°, $Re_\tau = 1142$) with $z_{ref} \approx 200$, contour levels -0.15 to 0.95 increments of 0.1 (Negative shown dashed); (b) outer-scaled variation of $l_y(R_{uu})$ with z_{ref} for ($\times$) $Re_\tau = 793$; ($\circ$) $Re_\tau = 1142$; ($\Diamond$) $Re_\tau = 2030$; ($\triangle$) $Re_\tau = 3071$

to these two regimes as 'coupled' (events at z_{ref} are still strongly influencing or influenced by the wall) and 'decoupled' (a noticeable decorrelation between fluctuations at z_{ref} and those at the wall). Whilst this decoupling point varies with contour level, the actual 'lift-off' occurs at a consistent z_{ref}/δ for any given contour (the decoupling point scales with outer variables). As an example, the $R_{uu} = 0.3$ contour decouples from the wall at $z_{ref}/\delta = 0.2$ (the approximate edge of the log region) for all Reynolds numbers tested. It is believed that these results indicate a general separation of hairpin-type structures (and hence reduction in wall-influence or feedback) as they grow beyond the logarithmic region.

The authors gratefully acknowledge support from the National Science Foundation (grant CTS-0324898) and the David and Lucile Packard Foundation.

References

[1] Balint, J-L., Wallace, J.M., Vukoslavcevic, P., 1991, *J. Fluid Mech.* **228**, 53-86

[2] Ganapathisubramani, B., Hutchins, N., Hambleton, W.T., Longmire, E.K., Marusic, I., 2004, *J. Fluid Mech.* , submitted

[3] Head, M. R. & Bandyopadhyay, P., 1981, *J. Fluid Mech.* **107**, 297-338

[4] Ganapathisubramani, B., Longmire, E.K., Marusic, I., 2003 *J. Fluid Mech.* **478**, 35-46

[5] Tomkins, C. D., Adrian, R. J., 2003, *J. Fluid Mech.* **490** 37-74

[6] Wark, C.E., Naguib, A.M., Robinson, S.K., 1991, *AIAA-paper* **91-0235**

[7] Mclean, I.R., 1990, PhD Thesis, University of Southern California, USA

[8] Marusic, I. & Perry, A.E. 1995 *J. Fluid Mech* **298**, 389–407.